Title

Rectification of Ion Current in Nanopores Depends on the Type of Monovalent Cations: Experiments and Modeling

Journal

The Journal of Physical Chemistry C, 118(18)

ISSN

1932-7447

Authors

Gamble, Trevor
Decker, Karl
Plett, Timothy S
et al.

Publication Date

2014-05-08

DOI

10.1021/jp501492g

Peer reviewed

THE JOURNAL OF PHYSICAL CHEMISTRY C

Article

pubs.acs.org/JPCC

Rectification of Ion Current in Nanopores Depends on the Type of Monovalent Cations: Experiments and Modeling

Trevor Gamble,[†] Karl Decker,[‡] Timothy S. Plett,[†] Matthew Pevarnik,[†] Jan-Frederik Pietschmann,[§] Ivan Vlassiouk,[∥] Aleksei Aksimentiev,*[,‡] and Zuzanna S. Siwy*[,†,⊥,#]

[†]Department of Physics and Astronomy, University of California, Irvine, Irvine, California 92697, United States

[‡]Department of Physics, Beckman Institute, University of Illinois, Urbana, Illinois 61820, United States

[§]Numerical Analysis and Scientific Computing, TU Darmstadt, Germany

[∥]Oak Ridge National Laboratory, Oak Ridge, Tennessee 37831, United States

[⊥]Department of Chemistry and [#]Department of Biomedical Engineering, University of California, Irvine, California 92697, United States

Supporting Information

ABSTRACT: Rectifying nanopores feature ion currents that are higher for voltages of one polarity compared to the currents recorded for corresponding voltages of the opposite polarity. Rectification of nanopores has been found to depend on the pore opening diameter and distribution of surface charges on the pore walls as well as pore geometry. Very little is known, however, on the dependence of ionic rectification on the type of transported ions of the same charge. We performed experiments with single conically shaped nanopores in a polymer film and recorded current−voltage curves in three electrolytes: LiCl, NaCl, and KCl. Rectification degrees of the pores, quantified as the ratio of currents recorded for voltages of opposite polarities, were the highest for KCl and the lowest for LiCl. The experimental observations could not be explained by a continuum modeling based on the Poisson−Nernst−Planck equations. All-atom molecular dynamics simulations revealed differential binding between Li^+, Na^+, and K^+ ions and carboxyl groups on the pore walls, resulting in changes to both the effective surface charge of the nanopore and cation mobility within the pore.

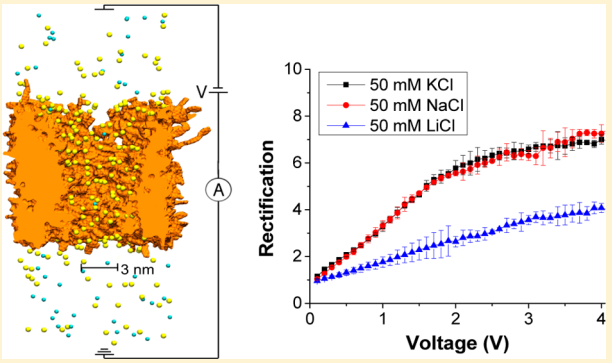

I. INTRODUCTION

Many experimental and theoretical groups have dedicated efforts to studying fundamental phenomena governing transport at the nanoscale as well as pioneering devices using nanoscale effects.[1,2] Rectification of ion current with nanopores is an example of transport properties stemming from the nanoscale openings of the structures.[3−7] Rectifying nanopores feature ion currents that are higher for voltages of one polarity compared to currents recorded for voltages of the same absolute values but of opposite polarity. They can thus work as switches for ions and charged molecules in solutions and could become the basis for ionic circuits used in logic and sensory systems.[8−11]

There have been a number of rectifying systems reported thus far. Glass pipettes[5,12] and tapered cone shaped nanopores with negative surface charges[6,13,14] were reported to be cation selective and conduct current with the preferential direction of the cation flow from the narrow opening to the wide base of the pore. Current−voltage curves of the pores were found to depend on the geometric characteristics of the small opening, the length of the pore, and the surface charge density of the pore walls.[15−23] Rectification properties of ionic systems were significantly improved by introducing surface charge patterns in which two zones of the pore walls were characterized by different surface characteristics.[8,24−30] In a bipolar diode, there is a zone with positive surface charges in contact with a zone with negative surface charges; a unipolar diode contains a junction between a zone that is charged and a zone that is neutral. Both types of ionic diodes were able to suppress ionic flow in one direction almost entirely so that the currents for one polarity were hundreds of times higher than currents for the voltages of opposite polarity.[25,26,28,30]

Fewer studies, however, have been performed on how rectification depends on the type of transported ions. The influence of cation charge has been reported for both man-made[31,32] and biological pores.[33−36] As an example, rectification of conically shaped, negatively charged polymer nanopores in KCl was compared with recordings in calcium and cobalt(III) ions.[32] The multivalent ions were shown to induce the effect of charge inversion;[37,39] i.e., in their presence, originally negatively

Received: February 11, 2014
Revised: March 24, 2014
Published: April 14, 2014

charged pore walls became effectively positively charged. Charge inversion was observed as a qualitative change in the current−voltage curves, suggesting the pores became anion selective.

Much less is known on whether ions with the same charge state can have differing influence on ion transport through nanopores. One study explored rectification of the bacterial pore α-hemolysin in various monovalent chloride salts;[40] pore rectification was strongest in CsCl and weakest in LiCl, and the difference was attributed to interactions of lithium ions with negatively charged groups on the pore walls. A similar question, as to the importance of type of monovalent cations for the rectification of man-made nanopores, has not yet been asked. The opening diameters of man-made structures are often significantly larger than the narrowest constriction of the α-hemolysin pore. Understanding transport of various cations in pores characterized with different opening diameters will provide insight into which interactions between ions and surfaces influence and determine properties of ionic transport through nanopores. This question is especially timely, since type of cation has also been reported to influence detection of DNA molecules using nanopores in the resistive pulse technique.[41] Studying interactions of ions with surfaces and walls in model nanopores is therefore important for understanding electrostatics at the nanoscale as well as making better nanopore sensors.

Ion transport through nanopores in contact with monovalent salts such as KCl, NaCl, and LiCl is typically described using continuum models based on the Poisson−Nernst−Planck equations.[15,42−47] Ions are treated as point charges and their interactions with charges on the walls are captured by the Poisson−Boltzmann equation. In this article we show limited application of this approach for the description of ionic transport through rectifying polymer nanopores in different monovalent salts.

First we present experimental observations of ion current rectification of single conically shaped nanopores with opening diameters between 3 and 25 nm, measured in KCl, NaCl, and LiCl. The measurements indicate the pores exhibit significantly lower rectification degrees in the lithium salt compared to the rectification in potassium and sodium chloride. The experimental findings are explained by all-atom simulations performed by molecular dynamics (MD) tools. We use a modified version of the all-atom representation of a polymer pore created in ref 48 to reveal the effects of differential ion binding to surface charged groups of identical poly(ethylene terephthalate) (PET) nanopores in KCl, NaCl, and LiCl solutions. We assess the dependence of rectification on the effective surface charge densities modulated by KCl, NaCl, and LiCl.

II. METHODS

Preparation of Nanopores. Single conically shaped nanopores were prepared in 12 μm thick films of PET using the track-etching technique.[49] Briefly, the films were irradiated with single Au or U ions accelerated to 11.4 MeV/u at the UNILAC linear accelerator of the GSI Helmholtzzentrum für Schwerionenforschung in Darmstadt, Germany.[50] In the next step, the irradiated films were subjected to wet chemical etching performed in a homemade conductivity cell. One side of the film was in contact with 9 M NaOH, while the other chamber of the conductivity cell was filled with an acidic stopping medium. This asymmetric etching procedure was reported before to result in conically shaped nanopores.[6,13]

Nanopore Characterization and Ion Current Measurements. After the etching had been completed, the membranes were rinsed with the stopping solution and water. The chambers of the conductivity cell were filled with 1 M KCl, and two homemade Ag/AgCl electrodes were used to record a current−voltage curve. The small opening of the nanopore was estimated based on the linear portion of the recording and approximating the pore shape with a truncated cone.[13] The large opening diameter created at the side that had been in contact with NaOH could be found based on the rate of nonspecific etching of PET in the etchant and time of etching.[13] Diameters of pores used in this study were 3−25 and 300−750 nm for the small and large opening, respectively.

Once the pore opening diameters were characterized, transport properties of each pore were measured in KCl, NaCl, and LiCl in the concentration range 10−200 mM. The side of the membrane with the large opening was in contact with a working electrode; the other side was grounded (Figure 1).

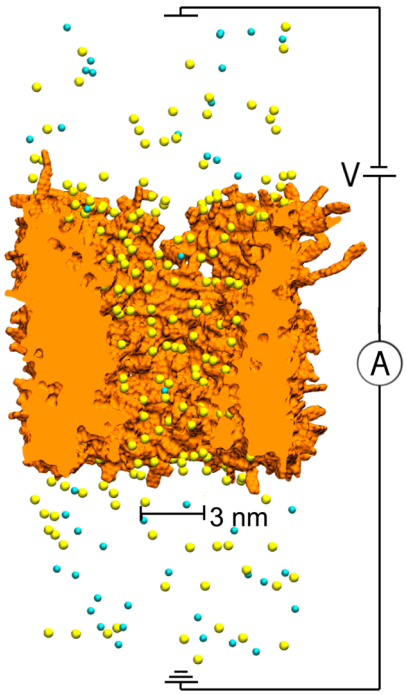

Figure 1. All-atom representation of a conical PET nanopore in contact with 0.1 M NaCl solution. Sodium and chloride ions are depicted as yellow and teal spheres, respectively; water is not shown. PET membrane is shown in orange. The nanopore tip is 3 nm in diameter as measured at the PET edge. The circuit diagram visualizes the electrode configuration used in experiments and in simulation; for negative applied voltages, cations move from the tip (shown at the bottom) toward the wider opening of the pore.

Continuum Modeling of Ion Currents. Ion current through a single conically shaped nanopore with opening diameters of 10 nm (the tip) and 1000 nm (the wide opening) was modeled by numerically solving the Poisson−Nernst−Planck (PNP) equations. We used a recently developed software package MsSimPore, shown to be especially powerful in modeling pores with high surface charge densities.[18] Although MsSimPore is based on 1D reduction of the PNP

dx.doi.org/10.1021/jp501492g | J. Phys. Chem. C 2014, 118, 9809−9819

model, it still allows for an explicit treatment of the electrolyte reservoirs in contact with the membrane.

Setup of MD Systems. All-atom representation of a conical PET nanopore was adapted from a model designed previously[48] with surface charge density of −1 e/nm^2, appropriate to simulate conditions at pH 7. Deletion of residues inside a geometric cone aligned with the existing hourglass-like pore resulted in a conical pore with an opening angle of ∼15° (Figure 1). The pore was 3 nm wide at the tip and 5 nm wide at the base, embedded in a PET membrane that was 10 nm long, 8 nm wide, and 11 nm deep with periodic boundary conditions to simulate an extended membrane. This small system size, as compared to the 12 μm long pores used in experiments, enabled us to run simulations for long times (tens of nanoseconds) without exceeding reasonable limits for required supercomputing resources. The membrane was then solvated using VMD's solvate plugin. Ions were added by replacement of randomly selected water molecules as necessary to neutralize the charge on the membrane and reach 0.1 M concentration in the bulk solution. Three such systems were created to separately simulate the nanopore in LiCl, NaCl, and KCl solutions. The size of the simulation-ready system was 26 nm × 8 nm × 11 nm and consisted of 221 778 atoms, including PET membrane and electrolyte solution. Additional three systems consisting solely of 0.1 M bulk solution (KCl, NaCl, or LiCl) were prepared, each of dimensions 26 nm × 8 nm × 11 nm with total of 220 542 atoms.

Protocols of MD Simulations. All MD simulations were performed using molecular dynamics program NAMD[51] and with CHARMM36[52] parameters for atomic interactions supplemented by NBFix corrections to accurately describe ion−PET interactions.[53] Particle mesh Ewald full electrostatics computed over a cubic grid with spacing <1 Å and a smooth (10−12 Å) cutoff for van der Waals interactions were implemented. We used 2 fs time step, rigid hydrogen bonds, and periodic boundary conditions. The temperature was held constant using the Lowe−Andersen thermostat,[54] rate 50 ps^{-1}, at 295 K. The TIP3P water model[55] was used in each simulation. Relative restraints, where necessary to maintain PET membrane integrity at the surface, were enforced using the extrabonds feature of NAMD and applied harmonic restraints between single carbon atoms of neighboring PET residues; the spring constant of each restraint was 0.2 kcal mol^{-1} Å^{-2}. Upon assembly, each system was minimized using the conjugate gradient method. The systems were then equilibrated for 0.5 ns in the NPT ensemble (constant number of particles N, constant pressure P, and constant temperature T) at 1 atm pressure enforced by the Langevin piston[56] extendible along the pore axis, with decay and period of 800 fs. Each of the systems was then simulated in the NVT ensemble (constant number of particles N, volume V, and temperature T) at a 2 V transmembrane bias induced by applying an electric field perpendicular to the membrane or along the longest axis for the bulk electrolyte systems. PET nanopore in each of KCl, NaCl, and LiCl was modeled for both polarities of the bias for 20 ns; the three bulk electrolyte systems were simulated for 20 ns each with only one polarity. 20 ns simulations in the absence of an external voltage bias further characterized the PET nanopore in the presence of the three salts. In each simulation of the PET nanopore, ionic current and distribution of ions throughout the system reached a steady state within the first 6 ns of the simulations; our analysis uses only the remainder of each trajectory. Enabling the zeroMomentum parameter in NAMD prevented aberrant acceleration of the electro-osmotic flow, and postsimulation realignment of the PET membrane removed the effects of the system drift from the simulation results. Because of the low polarizability of the material, no special arrangements were made to match the dielectric polarizability of the simulated PET membrane.[57] Visualization and analysis were performed using VMD.[58]

III. RESULTS AND DISCUSSION

Figure 2 presents example current−voltage curves of two single conically shaped nanopores recorded in 50 mM solutions of

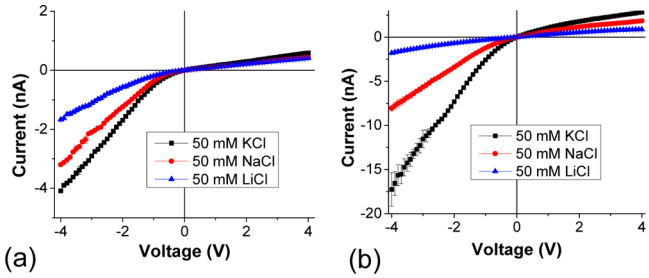

Figure 2. Example current−voltage curves of single conically shaped nanopores with opening diameters of (a) 9 and (b) 14 nm. The recordings were performed in 50 mM solutions of KCl, NaCl, and LiCl. Average values of three scans are presented.

KCl, NaCl, and LiCl. The magnitude of the currents changes in accordance with the ionic mobility; among KCl, NaCl, and LiCl, lithium has the lowest mobility and consequently, the currents in LiCl were the lowest among the recordings in the three salts. The experiments were performed at pH 8 at which the pore walls carry negative surface charge due to deprotonated carboxyls. Charge density of the pore walls of −1 e/nm^2 was estimated based on measurements of pore conductance at a wide range of KCl concentrations between 1 mM and 1 M and ion conductance saturation at low ionic strengths.[59−61] The measurements were performed for a cylindrical pore however preparation of pores of any geometry in PET involves etching irradiated foils in NaOH. Thus, we assumed the value of −1 e/nm^2 to be valid for tapered cone-shaped pores as well. For simplicity, we also assumed the charge density was uniform throughout the whole length of the pore.

The recordings in Figure 2 also indicate the examined pores rectified ion current with the preferential direction of cation flow from the tip to the wide opening (base) of the cone. Current rectification in KCl of conically shaped nanopores was examined in detail before and explained via voltage dependence of ionic concentrations in the pore.[42,43,45−47,53,62,63] At the forward bias (negative voltages in our experimental setup), concentration of both cations and anions increases above the bulk concentration, leading to a nonlinear current enhancement. As a result, negative currents are carried by both types of ions, and the pores at the forward bias are only weakly cation selective.[18,42] At the reverse bias (positive voltages in our electrode configuration), the ionic flow is limited by the formation of a depletion zone, whose width increases with the increase of reverse bias.[18] The depletion zone contains mostly cations; thus, positive currents can be treated as cationic currents only. Rectification properties of nanopores are often described by a rectification degree defined as a ratio of currents

dx.doi.org/10.1021/jp501492g | J. Phys. Chem. C 2014, 118, 9809−9819

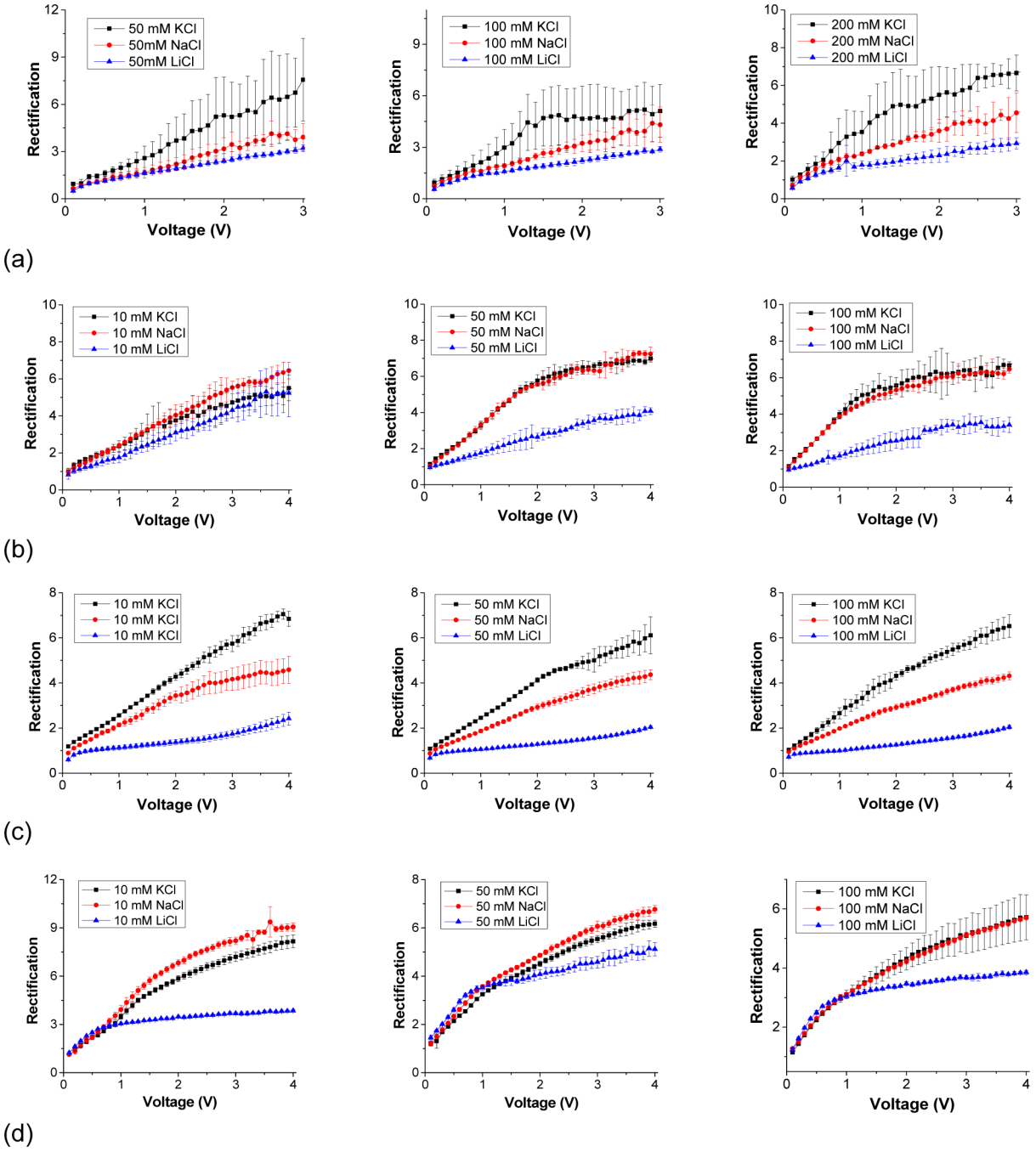

Figure 3. Rectification degrees of single conically shaped nanopores with opening diameters of (a) 4 and 350 nm, (b) 9 and 300 nm, (c) 14 and 520 nm, and (d) 22 and 570 nm. The 4 nm pore exhibited large fluctuations of ion current in 10 mM of KCl, NaCl, and LiCl and above 3 V for all other studied concentrations; thus, data for 50, 100, and 200 mM in the voltage range between −3 and +3 V are presented. All remaining structures were analyzed in the voltage range −4 to +4 V. For each pore, rectification degrees for three KCl, NaCl, and LiCl concentrations are shown.

recorded at a given magnitude of voltage but of opposite polarities.

We were, however, surprised to see that rectification degrees of conically shaped nanopores in LiCl were consistently lower compared to the recordings in KCl (Figure 3). This effect was observed in pores with a wide range of opening diameters between 3 and 25 nm. The difference in rectification properties in LiCl versus KCl was most pronounced in the range of salt concentrations between 50 and 200 mM. Four out of seven examined pores also differentiated between KCl and NaCl, i.e., rectification degrees in NaCl fell between rectification degrees in KCl and LiCl; the four structures included three with sub-5 nm opening diameter. For the 22 nm pore, the lower rectification degrees observed in LiCl became pronounced only at voltages above ∼1 V (Figure 3d); this behavior was reproduced in a 25 nm pore (Supporting Information). We explain this observation by voltage-dependent enhancement of ionic concentrations in conical pores at negative voltages. For pores with a wider opening, larger magnitudes of voltage need to be applied to get a similar enhancement of cation and anion concentrations compared to the enhancement in narrower pores (Supporting Information).[15,42] The experiments suggest

dx.doi.org/10.1021/jp501492g | J. Phys. Chem. C 2014, 118, 9809−9819

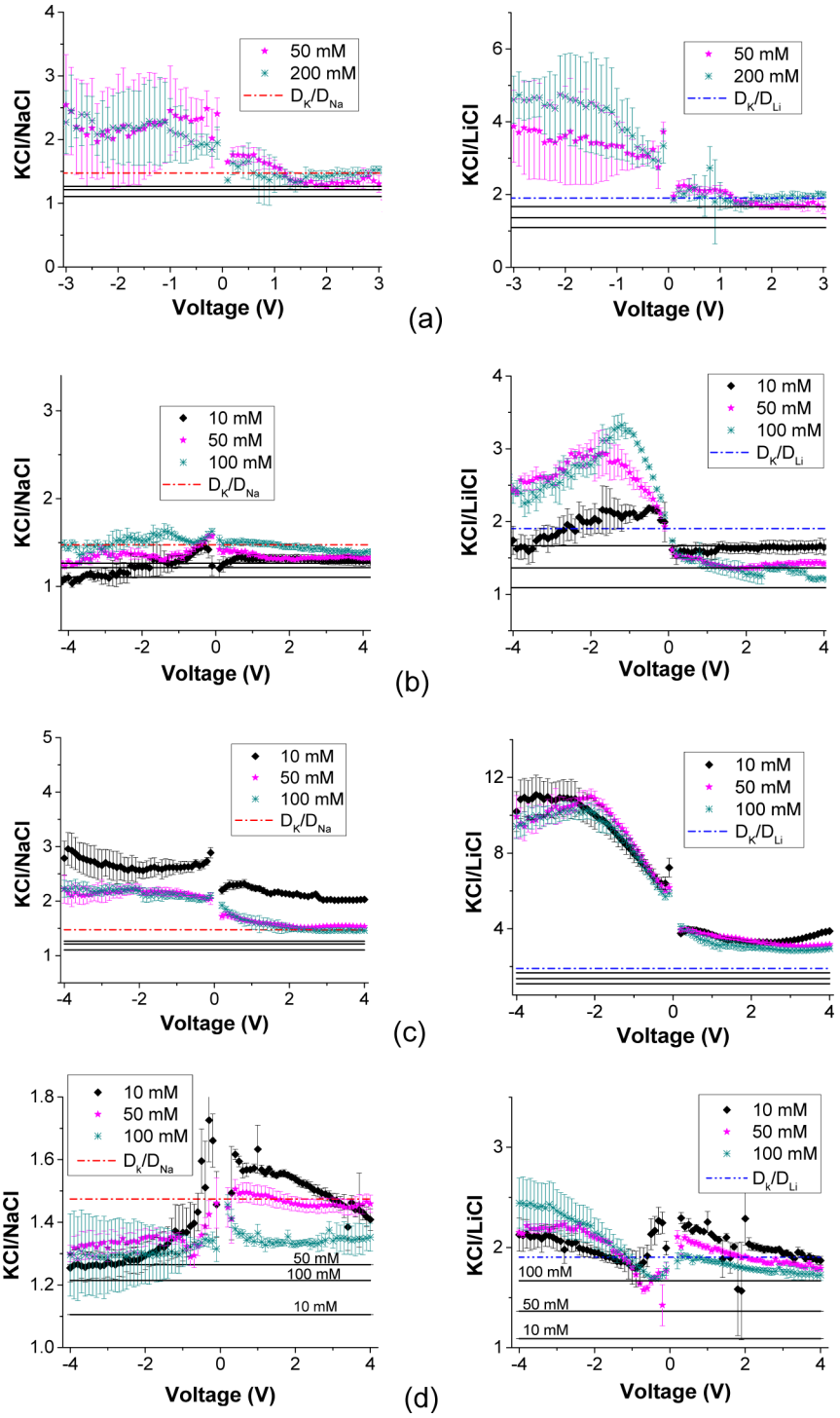

Figure 4. Ratios of ion currents recorded in KCl and NaCl (KCl/NaCl) and KCl and LiCl (KCl/LiCl) for single pores with an opening diameter of (a) 4, (b) 9, (c) 14, and (d) 22 nm. Ratios of diffusion coefficient, *D*, of cations are indicated as dotted lines. Ratios of bulk conductivities are shown as black lines labeled in (d).

concentration of accumulated lithium ions in the pore has to reach a critical value to reduce the magnitude of negative currents and ion current rectification.

We would also like to point to a weak dependence of the rectification degree on electrolyte concentration and pore opening diameter observed for sub-20 nm pores (Figure 3). An existence of a range of concentrations with similar rectification degrees was reported before and explained by the formation of the depletion zone even in pores whose opening diameter is several times larger than the Debye length.[18,42] The dependence of ion current rectification on electrolyte concentration and pore diameter has a broad maximum because a depletion zone cannot be fully created if the Debye length overlap occurs over a significant portion of a pore. This leads to the nonintuitive observation of similar rectification properties of pores with a wide range of opening diameter, reported for KCl before.[42] The increase of rectification degree in LiCl with voltage is weaker than in the case of sodium and potassium

dx.doi.org/10.1021/jp501492g | J. Phys. Chem. C 2014, 118, 9809−9819

salts, again suggesting that accumulation of lithium ions in the pore might interfere with further enhancement of cation and anion concentrations.

It is important to mention that each conically shaped nanopore even with the same tip diameter is unique and different. Opening diameter of the base of the cone is determined by the etching time and for the set of pores used in this study varied between 300 and 750 nm. Rectification degree of conical pores was found dependent on the cone opening angle,[18] shape of the very tip of the pore,[17] and even atomistic details of the pore walls.[7] Thus, by presenting data of four pores, we emphasize the qualitative reproducibility of lower rectification degrees in LiCl compared to KCl and quantitative variability of the magnitude of the effect. Additional data for three nanopores are shown in the Supporting Information.

In order to understand the origin of the dependence of rectification degree on type of salt, we looked first at ratios of ion currents recorded in KCl and NaCl as well as KCl and LiCl; the obtained values were compared with ratios of bulk conductivities of the salts κ ($\kappa_{KCl}/\kappa_{NaCl}$ and $\kappa_{KCl}/\kappa_{LiCl}$) as well as ratios of diffusion coefficients of the cations. The pore with 4 nm opening diameter was unstable at voltages beyond 3 V. Thus, only data for lower voltages were considered for this sample; the remaining pores were analyzed in the voltage range of −4 and +4 V (Figure 4). Some rectifying nanopores with small opening diameters were shown before to exhibit intrinsic current fluctuations.[62,64,65] As a consequence, current ratios for the 4 nm pore also have the largest error bars, especially pronounced in KCl. Smaller variation of currents in NaCl and LiCl might be related with their lower rectification degrees, suggesting lower electric fields at the pore tip compared to the case in KCl. Concentration of electric field at the narrow opening was suggested to lead to current instabilities.[64] Because of the fluctuating current signal and large error bars of the current ratios, values in only two salts concentrations are shown for the 4 nm pore (Figure 4a). For nearly all examined pores, the ratio of negative currents in KCl and in LiCl was significantly higher than it would be expected from the ratio of bulk conductivities or diffusion coefficients. This finding indicates the currents of nanopores in LiCl were reduced compared to the predictions based on the bulk solution behavior, treating the recordings at KCl as a reference point. The ratio of negative currents in KCl and LiCl varied between different pores and was as high as 10 and as low as ∼3 for 4 V; the ratio of positive currents was often close to the ratios of diffusion coefficients or bulk conductivities (Figure 4). The difference in currents in KCl and NaCl was typically voltage-independent and smaller than in the case of KCl and LiCl.

In order to determine if the observed differences in rectification degrees and values of currents measured in KCl, NaCl, and LiCl can be explained by the differences in diffusion coefficients of potassium, sodium, and lithium ions, ion transport in conical pores was modeled using the continuum approach based on the Poisson−Nernst−Planck equations.[15,18] The purpose of the simulations was not to quantitatively fit the experimental data but rather check if the continuum approach predicts the lowest rectification in LiCl. The model did not include Navier−Stokes equations; thus, electroosmosis was not taken into account. Conically shaped nanopipettes were shown to produce polarity-dependent electroosmotic fluid flow;[66] however, our earlier numerical modeling of rectifying nanoporous systems indicated the influence of electroosmosis on ion current rectification was small.[67] The modeling was performed for a tapered cone pore with opening diameters of 10 and 1000 nm and surface charge density of −1 e/nm^2. We used the recently developed software package MsSimPore, which uses a Newton scheme to discretize the PNP equations.[18] The surface charge density was kept constant in all simulations. Ions were treated as point charges, and their diffusion coefficients in the pore were assumed to be equal to their values in a bulk solution found in the literature. We justified the choice by an almost linear dependence of the salts' bulk conductance on concentration up to 2 M. Figure 5 presents modeled

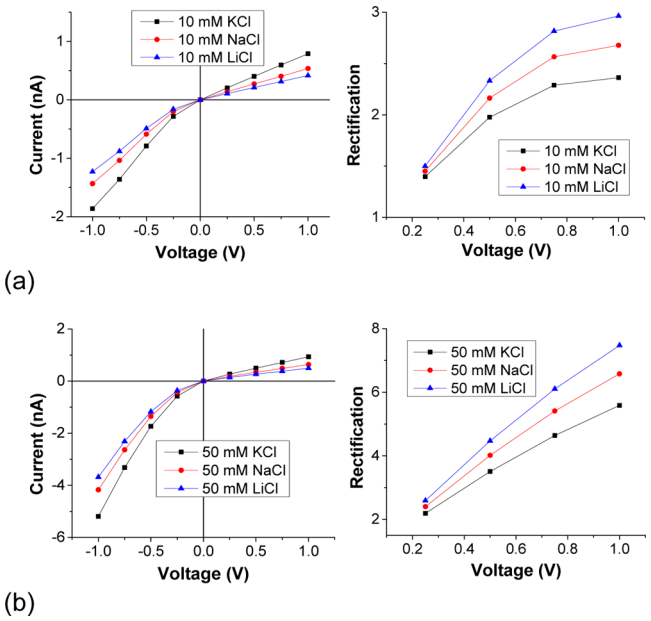

Figure 5. Ion currents predicted by the Poisson−Nernst−Planck equations solved numerically for a single conically shaped nanopore with opening diameters of 10 nm (tip) and 1000 nm (base). The surface charge density of the pore walls was set to −1 e/nm^2. Current−voltages curves and rectification degrees are shown in (a) for 10 mM and (b) 50 mM KCl, NaCl, and LiCl.

current−voltage curves and resulting rectification degrees for LiCl, NaCl, and KCl. The model indeed captured the rectification effect observed with conically shaped nanopores and the lowest values of currents in LiCl. The continuum approach, however, could not reproduce the lowest rectification degrees experimentally observed in the lithium salt. In fact, the continuum modeling predicted a modest increase of rectification in LiCl compared to KCl.

We also plotted the ratio of PNP modeled currents in KCl and LiCl and KCl and NaCl in a range of voltages between −1 and +1 V (Figure 6). Our experiments showed the ratios of ion currents in KCl and LiCl to be higher for negative voltages compared to the ratios at positive voltages, while the continuum modeling predicted an opposite voltage dependence. The modeled data can be understood taking into account voltage-dependent ionic selectivity of conically shaped pores.[18,42] Positive currents are primarily carried by positive ions thus the ratio of the modeled currents in KCl and LiCl (or KCl and NaCl) corresponds to the ratio of diffusion coefficients of potassium and lithium ions (potassium and sodium). At negative voltages, the pore lumen is filled with both cations and anions; thus, the ratio of currents approaches the ratio of bulk conductivities in 50 mM KCl. In 10 mM KCl, the ratio of

dx.doi.org/10.1021/jp501492g | J. Phys. Chem. C 2014, 118, 9809−9819

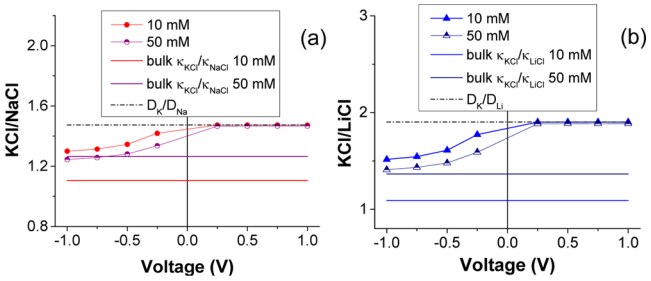

Figure 6. Ratio of ion currents predicted by the continuum modeling based on the Poisson−Nernst−Planck equations solved for a single conically shaped nanopore in (a) KCl and NaCl and (b) KCl and LiCl. Ratios of bulk conductivities ($\kappa_{KCl}/\kappa_{NaCl}$ and $\kappa_{KCl}/\kappa_{LiCl}$) in 10 and 50 mM as well as of diffusion coefficients D are also indicated. Opening diameters of the modeled conical pore were 10 and 1000 nm.

transmembrane negative currents is higher than in bulk likely due to large enhancement of ionic concentrations in the pore.[18]

The continuum modeling was performed assuming the surface charge density of nanopores was not affected by the concentration or type of salt solution. Both the ion current rectification of conically shaped pores and ion current values in all nanopores are known to be modulated by the electrical surface characteristics.[6,15,18,21] We therefore hypothesized the experimental results in LiCl could be explained if lithium ions lowered the effective surface charge of the pores.

Lithium ions were recently found to reduce ion current rectification in a bacterial pore of α-hemolysin (α-HL).[40] Although α-HL is weakly anion selective,[68−71] it has 63 carboxyl groups along the ionic path. All-atom molecular dynamics simulations revealed that differential affinities of cations to carboxyls are responsible for the reduction of current and rectification.[40] Better screening of negatively charged residues by lighter monovalent ions reduced the effective charge of the pore opening and consequently the degree of ion current rectification. In contrast to α-HL, the polymer pores considered here are cation selective, and the pore walls are covered with carboxyl groups at a high density of ∼1 per nm^2. The effect of lithium ions on ion current values and rectification was a few times more pronounced compared to the effect measured in α-HL.

In order to elucidate the microscopic phenomena underlying differential rectification of ionic current in polymer nanopores, a set of MD simulations were performed utilizing an all-atom representation of a PET nanopore.[48] The primary goal of the simulations was to test for the differential binding of monovalent ions to charged pore walls. It is important to mention the MD model captured both electrophoretic and electroosmotic effects on ions and water. All simulations were performed at pH 7, which corresponded to the surface charge density of −1 e/nm^2. Each system measured 26 nm × 8 nm × 11 nm and contained a 10 nm thick PET membrane in 0.1 M LiCl, NaCl, or KCl solution. After equilibration, each of the three systems was simulated at 2 V of both polarities as well as in the absence of the external bias for a total of nine simulations of 20 ns length each. The coordinates of the system were recorded every 6000 frames, or 12 ps, to enable detailed analysis of the system dynamics and building trajectories of all ions.

Analysis of the trajectories revealed cations would bind to the PET membrane surface, resulting in the reduction of the effective surface charge density on the pore walls (Figure 7). An

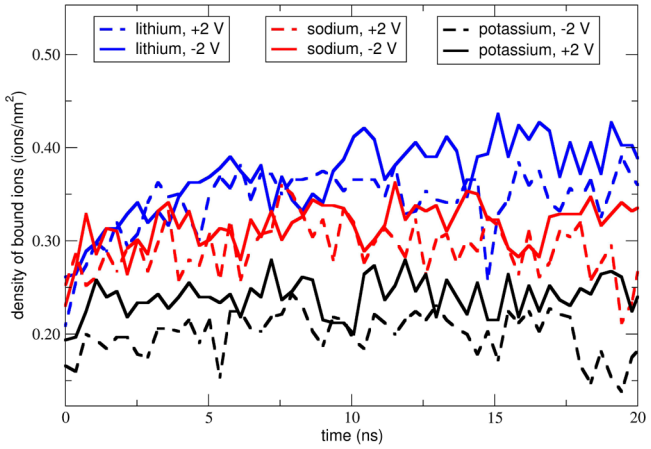

Figure 7. Density of cations bound to PET pore walls vs simulation time for each of the nine performed MD simulations with KCl, NaCl, and LiCl at 2 V of both polarities. Zero on the x-axis corresponds to the beginning of the production MD simulation run. Number of bound lithium ions increases in the first ∼10 ns when it saturates and exhibits fluctuations around a steady average value.

ion was considered bound if it remained within 7 Å of the pore wall and failed to move a minimum distance expected due to diffusion. To find the number of bound ions as a function of time, we performed a frame-by-frame analysis of each cation's position, calculated the minimum expected cation displacement due to diffusion between frames, and compared it with the actual displacement. Initial estimates of the minimum expected displacement, r, were found using the formula $r = (6D\Delta t)^{1/2}$, where D is the diffusion coefficient of an ion and Δt is the considered time interval. We assumed values of D of 1.1, 1.4, and 2.0 nm^2/ns for lithium, sodium, and potassium ions, respectively, which are close to the experimental values for dilute solutions.[72] Further validation of the model revealed that sampling cations' position every 30 recorded frames, or $\Delta t \approx$ 0.36 ns, and using a minimum expected displacement of 4−8 Å, resulted in an average number of bound cations at any given step that was insensitive to small parameter changes. The requirement that ions have to be within a certain distance from the surface to be considered bound was found to exclude only 1% of cations otherwise expected to be bound.

The number of bound ions was subsequently used to calculate the effective surface charge density of the pore walls in the presence of the three salts (Table 1 and Figure 7). The simulations indicated Li^+ ions neutralized a higher fraction of the PET surface charge compared to Na^+ or K^+ ions. These results indeed explain the experimental observation of the dependence of rectification degree on the type of electrolyte. Ion current rectification of conically shaped nanopores is known to be modulated by the surface charge density.[15,18]

Table 1. Effective Surface Charge Density σ at the Membrane−Solution Interface As Determined by MD Simulations[a]

type of electrolyte, 0.1 M	σ (e/nm^2) at −2 V	σ (e/nm^2) at zero bias	σ (e/nm^2) at 2 V
LiCl	−0.64 ± 0.01	−0.61 ± 0.01	−0.66 ± 0.01
NaCl	−0.70 ± 0.01	−0.67 ± 0.01	−0.72 ± 0.01
KCl	−0.78 ± 0.01	−0.77 ± 0.01	−0.82 ± 0.01

[a]Without ion binding, the surface charge density is σ = −1.0 e/nm^2.

dx.doi.org/10.1021/jp501492g | J. Phys. Chem. C 2014, 118, 9809−9819

There is a range of surface charge densities where the decrease in the number of charged groups leads to the reduction of ion current rectification. Thus, it is expected that LiCl currents will be rectified least when compared with the rectification in KCl and LiCl.

The performed MD simulations and effective surface charge reduction observed with NaCl and LiCl can also explain why only a subset of studied pores showed differences in rectification in NaCl and KCl; in all studied pores, rectification in LiCl was the lowest. For high surface charge densities, the dependence of rectification on surface charge is relatively weak; thus, the reduction of the surface charge by sodium cannot always be detected as a change in rectification.[18]

Interestingly, the two largest pores examined in this study with the opening of 22 and 25 nm exhibited the highest rectification degrees in NaCl and not KCl, following predictions of the continuum modeling. We do not have yet explanation for that effect.

The performed simulations also allowed us to quantify transmembrane currents carried by each type of ion. In contrast to experimental observations, ion currents obtained from MD simulations exhibit an opposite rectification; i.e., positive currents are higher in magnitude than negative currents (Tables 2 and 3). The discrepancy between the MD and experimental results stems most probably from the dimensions of the PET pore used in the all-atom simulations. A prior analysis revealed that the formation of a depletion zone for positive voltages, and enhancement of ionic concentrations for negative voltages occurred only in pores that were at least 100 nm long, thus 10 times longer than the one used in our MD simulation system.[18,67]

Table 2. MD Simulated Ion Currents through a PET Nanopore

salt type	current-carrying ions	I (nA) at −2 V	I (nA) at 2 V
LiCl	LiCl	−4.49 ± 0.06	6.70 ± 0.05
	Li^+	−4.26 ± 0.06	6.07 ± 0.05
	Cl^-	−0.22 ± 0.04	0.63 ± 0.03
NaCl	NaCl	−4.62 ± 0.06	6.44 ± 0.06
	Na^+	−4.39 ± 0.06	6.21 ± 0.05
	Cl^-	−0.23 ± 0.03	0.23 ± 0.03
KCl	KCl	−6.63 ± 0.07	10.08 ± 0.06
	K^+	−6.57 ± 0.07	10.00 ± 0.07
	Cl^-	−0.06 ± 0.04	0.08 ± 0.04

Table 3. Rectification Degrees of a PET Nanopore Modeled by MD[a]

salt type	current-carrying ions	$I_{-2\ V}/I_{+2\ V}$
LiCl	LiCl	0.670 ± 0.007
NaCl	NaCl	0.719 ± 0.007
KCl	KCl	0.658 ± 0.006

[a]Note that rectification degrees less than 1 indicate rectification direction opposite to that observed in experiments.

Ionic distributions in the MD simulated PET pore are shown in Figure 8. The concentrations of mobile ions are enriched when cations are moving from the wide opening to the tip of the pore. Voltage modulation of ionic concentrations occurs near the tip: the density of mobile ions at −2 V is ∼3 times lower than the density at +2 V. Note: it is opposite to what is observed in long, conically shaped nanopores. We think the discrepancy in rectification of the MD simulated and long pores occurs due to possibly different mechanisms responsible for voltage modulation of ionic concentrations. In long pores, the depletion zone is created when potassium ions are sourced from the wide opening and thus when they have to be transported through a long resistive element to reach the pore tip where the cation concentration is dominated by the surface charge.[5,15,18,43,62] In a short pore, like the one modeled by MD, the access of cations to the pore tip can be limited by the small opening. It will be interesting to test experimentally the magnitude and direction of rectification of sub-20 nm long nanopores.

To provide further evidence ion currents in LiCl through conically shaped nanopores are reduced due to interactions of the ions with charges on the walls, we also simulated ion currents in bulk volumes of LiCl, NaCl, and KCl. We used the same voltage and salt concentrations as these in the PET nanopore simulations and calculated ratios of currents in the modeled bulk solutions and PET nanopore (Table 4). The simulations revealed a significant decrease of the current through the pore in LiCl compared to the reduction of the current observed in KCl. For both voltage polarities, the ratio of currents I_{KCl}/I_{LiCl} through the pore was significantly higher than the currents ratio obtained in bulk KCl and LiCl (Table 4). Thus, in accordance with experiments (Figure 4), our all-atom simulations suggest that interactions of lithium ions with the PET membrane reduce the nanopore conductance to a larger extent than in the case of potassium ions.

The findings were supported by calculating the ratio of diffusion coefficients of cations in the pore and in the bulk using simulated ionic trajectories. The diffusion coefficient of Li^+ in the pore was reduced by ∼50% compared to the value in the bulk. The reduction of diffusion coefficient for K^+ and Na^+ in the pore was smaller and equal to 30% and 40%, respectively.

IV. CONCLUSIONS

In this article we present experimental and modeling studies detailing the effect of three monovalent cations on ion current rectification of conically shaped nanopores. Our experimental findings were explained by molecular dynamics simulations of an all-atom representation of a model polymer PET pore. The simulations revealed the differences in ionic rectification of conical nanopores measured in LiCl, NaCl, and KCl resulted from differential binding of the cations to the PET membrane surface. The number of bound lithium ions was larger than the number of bound K^+ or Na^+. Consequently, lithium ions caused the most significant reduction of the effective surface charge density, and pores in LiCl showed the lowest rectification and currents. The reduction of lithium currents in the pore was larger than what could be predicted based on differences in bulk diffusion coefficients of K^+, Na^+, and Li^+ ions.

The results suggest that all-atom representation of nanopores can provide invaluable information helping to understand interactions between transported ions and pore walls. The continuum modeling based on PNP equations is sufficient to explain the effect of rectification but cannot capture properties of ionic current carried by different monovalent cations. It would be interesting to model ionic transport with coupled PNP and Navier−Stokes equations including the effect of induced charge electroosmosis[73] as well electroosmosis induced fluid flow instabilities.[74−76] Addition of the fluid flow effects might improve the agreement between the model predictions and experimental observations.

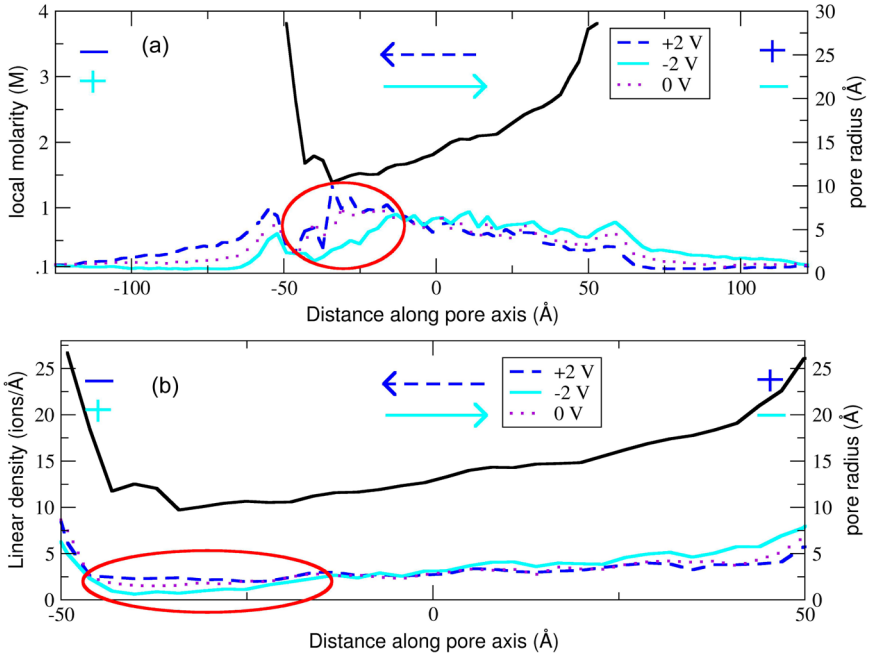

Figure 8. (a) Local molarity and (b) linear density of mobile ions along the nanopore axis obtained in MD simulations performed in 0.1 M LiCl. Plus and minus signs indicate polarity of the applied voltage, and arrows show the direction of cation flow in each case. Local pore radius along the axis is shown in (a) and (b) (black line, see right *y*-axis); regions beyond −50 and +50 Å are outside the pore. Red circle indicates the constriction of the pore, where a depletion zone forms at −2 V. The existence of the depletion zone was observed in KCl and NaCl solutions as well (not shown).

Table 4. Ratios of Ion Currents Obtained in MD Simulations for a PET Nanopore and Bulk Solutions

system conditions	I_{KCl}/I_{NaCl}	I_{KCl}/I_{LiCl}
−2 V, PET nanopore	1.43 ± 0.01	1.48 ± 0.01
+2 V, PET nanopore	1.56 ± 0.01	1.50 ± 0.01
bulk solution	1.21 ± 0.01	1.13 ± 0.01

Modulation of effective surface charge density by transported ions has very important implications for designing artificial ion selective membranes, ionic diodes, and ionic circuits. Reduction of surface charge density in nanopores by multivalent ions was shown before.[31,32,37−39] This study alerts researchers that monovalent ions can also modulate surface charge density of surfaces and influence functioning of ionic devices.

■ ASSOCIATED CONTENT

Supporting Information

Experimental data on ion current rectification for three additional nanopores as well as continuum modeling of ion currents for a pore with different opening diameters as these described in the article; voltage-dependent profiles of ionic concentrations in the pore. This material is available free of charge via the Internet at http://pubs.acs.org.

■ AUTHOR INFORMATION

Corresponding Authors

*E-mail aksiment@illinois.edu (A.A.).
*E-mail zsiwy@uci.edu (Z.S.S.).

Notes

The authors declare no competing financial interest.

■ ACKNOWLEDGMENTS

Irradiation with swift heavy ions was performed at the GSI Helmholtzzentrum für Schwerionenforschung GmbH, Darmstadt, Germany. T. Gamble, M. Pevarnik, and Z. Siwy were supported by the Nanostructures for Electrical Energy Storage, an Energy Frontier Research Center funded by the US Department of Energy, Office of Science, Office of Basic Energy Sciences (Award DESC0001160), and the National Science Foundation (CHE-1306058). K. Decker and A. Aksimentiev were supported by grants from the National Science Foundation (DMR-0955959) and the National Institutes of Health (R01-HG007406). The authors gladly acknowledge supercomputer time provided through XSEDE Allocation Grant MCA05S028 and the Blue Waters petascale computing facility at the University of Illinois. The authors are very grateful for many discussions with Prof. Phillip Collins and Prof. Reginald Penner from the University of California, Irvine.

■ REFERENCES

(1) Schoch, R. B.; Han, J.; Renaud, P. Transport Phenomena in Nanofluidics. *Rev. Mod. Phys.* **2008**, *80*, 839−883.
(2) Zhou, K.; Perry, J. M.; Jacobson, S. C. Transport and Sensing in Nanofluidic Devices. *Annu. Rev. Anal. Chem.* **2011**, *4*, 321−341.
(3) Siwy, Z. S. Ion Current Rectification in Nanopores and Nanotubes with Broken Symmetry Revisited. *Adv. Funct. Mater.* **2006**, *16*, 735−746.
(4) Siwy, Z. S.; Howorka, S. Engineered Voltage-Responsive Nanopores. *Chem. Soc. Rev.* **2010**, *39*, 1115−1132.
(5) Wei, C.; Bard, A. J.; Feldberg, S. W. Current Rectification at Quartz Nanopipet Electrodes. *Anal. Chem.* **1997**, *69*, 4627−4633.
(6) Siwy, Z.; Fulinski, A. Fabrication of a Synthetic Nanopore Ion-Pump. *Phys. Rev. Lett.* **2002**, *89*, 198103 (1−4).
(7) Cruz-Chu, E. R.; Aksimentiev, A.; Schulten, K. Ionic Current Rectification through Silica Nanopores. *J. Phys. Chem. C* **2009**, *113*, 1850−1862.
(8) Cheng, L.-J.; Guo, L. J. Ion Current Rectification, Breakdown, and Switching in Heterogenous Oxide Nanofluidic Devices. *ACS Nano* **2009**, *3*, 575−584.
(9) Ali, M.; Mafe, S.; Ramirez, P.; Neumann, R.; Ensinger, W. Logic Gates Using Nanofluidic Diodes Based on Conical Nanopores

Functionalized with Polyprotic Acid Chains. *Langmuir* **2009**, *25*, 11993−11997.
(10) Han, J.-H.; Kim, K. B.; Kim, H. C.; Chung, T. D. Ionic Circuits Based on Polyelectrolyte Diodes on a Microchip. *Angew. Chem., Int. Ed.* **2009**, *48*, 3830−3833.
(11) Tybrandt, K.; Forchheimer, R.; Berggren, M. Logic Gates Based on Ionic Transistors. *Nat. Commun.* **2012**, *3*, 871 (1−6).
(12) Umehara, S.; Pourmand, N.; Webb, C. D.; Davis, R. W.; Yasuda, K.; Karhanek, M. Current Rectification with Poly-l-Lysine-Coated Quartz Nanopipettes. *Nano Lett.* **2006**, *6*, 2486−2492.
(13) Apel, P. Yu; Korchev, Y. E.; Siwy, Z.; Spohr, R.; Yoshida, M. Diode-Like Single Ion-Track Membrane Prepared by Electro-Stopping. *Nucl. Instrum. Methods Phys. Res., Sect. B* **2001**, *184*, 337−346.
(14) Enculescu, I.; Siwy, Z.; Dobrev, D.; Trautmann, C.; Toimil-Molares, M. E.; Neumann, R.; Hjort, K.; Spohr, R. Copper Nanowires Electrodeposited in Etched Single-Ion Track Templates. *Appl. Phys. A: Mater. Sci. Process.* **2003**, *77*, 751−755.
(15) Cervera, J.; Schiedt, B.; Ramirez, P. A Poisson/Nernst-Planck Model for Ionic Transport through Synthetic Conical Nanopores. *Europhys. Lett.* **2005**, *71*, 35−41.
(16) Ali, M.; Yameen, B.; Cervera, J.; Ramirez, P.; Neumann, R.; Ensinger, W.; Knoll, W.; Azzaroni, O. Layer-by-Layer Assembly of Polyelectrolytes into Ionic Current Rectifying Solid-State Nanopores: Insights from Theory and Experiment. *J. Am. Chem. Soc.* **2010**, *132*, 8338−8348.
(17) Apel, P. Yu.; Blonskaya, I. V.; Orelovitch, O. L.; Ramirez, P.; Sartowska, B. A. Effect of Nanopore Geometry on Ion Current Rectification. *Nanotechnology* **2011**, *22*, 175302 (1−13).
(18) Pietschmann, J.-F.; Wolfram, M.-T.; Burger, M.; Trautmann, C.; Nguyen, G.; Pevarnik, M.; Bayer, V.; Siwy, Z. S. Rectification Properties of Conically Shaped Nanopores: Consequences of Miniaturization. *Phys. Chem. Chem. Phys.* **2013**, *15*, 16917−16926.
(19) Siwy, Z.; Heins, E.; Harrell, C. C.; Kohli, P.; Martin, C. R. Conical-Nanotube Ion-Current Rectifiers: The Role of Surface Charge. *J. Am. Chem. Soc.* **2004**, *126*, 10850−10851.
(20) Kovarik, M. L.; Zhou, K.; Jacobson, S. C. Effect of Conical Nanopore Diameter on Ion Current Rectification. *J. Phys. Chem. B* **2009**, *113*, 15960−15966.
(21) Sa, N.; Fu, Y.; Baker, L. A. Reversible Cobalt Ion Binding to Imidazole-Modified Nanopipettes. *Anal. Chem.* **2010**, *82*, 9963−9966.
(22) Yameen, B.; Ali, M.; Neumann, R.; Ensinger, W.; Knoll, W.; Azzaroni, O. Single Conical Nanopores Displaying pH-Tunable Rectifying Characteristics. Manipulating Ionic Transport with Zwitterionic Polymer Brushes. *J. Am. Chem. Soc.* **2009**, *131*, 2070−2071.
(23) Ali, M.; Ramirez, P.; Mafe, S.; Neumann, R.; Ensinger, W. A pH-Tunable Nanofluidic Diode with a Broad Range of Rectifying Properties. *ACS Nano* **2009**, *3*, 603−608.
(24) Daiguji, H.; Oka, Y.; Shirono, K. Nanofluidic Diode and Bipolar Transistor. *Nano Lett.* **2005**, *5*, 2274−2280.
(25) Vlassiouk, I.; Siwy, Z. S. Nanofluidic Diode. *Nano Lett.* **2007**, *7*, 552−556.
(26) Karnik, R.; Duan, C.; Castelino, K.; Daiguji, H.; Majumdar, A. Rectification of Ionic Current in a Nanofluidic Diode. *Nano Lett.* **2007**, *7*, 547−551.
(27) Maglia, G.; Heron, A. J.; Hwang, W. L.; Holden, M. A.; Mikhailova, E.; Li, Q.; Cheley, S.; Bayley, H. Droplet Networks with Incorporated Protein Diodes Show Collective Properties. *Nat. Nanotechnol.* **2009**, *4*, 437−440.
(28) Nguyen, G.; Vlassiouk, I.; Siwy, Z. S. Comparison of Bipolar and Unipolar Diodes. *Nanotechnology* **2010**, *21*, 265301 (1−8).
(29) Gracheva, M. E.; Vidal, J.; Leburton, J.-P. p-n Semiconductor Membrane for Electrically Tunable Ion Current Rectification and Filtering. *Nano Lett.* **2007**, *7*, 1717−1722.
(30) Yan, R.; Liang, W.; Peidong, Y. Nanofluidic Diodes Based on Nanotube Heterojunctions. *Nano Lett.* **2009**, *9*, 3820−3825.
(31) van der Heyden, F. H. J.; Stein, D.; Besteman, K.; Lemay, S. G.; Dekker, C. Charge Inversion at High Ionic Strength Studied by Streaming Currents. *Phys. Rev. Lett.* **2006**, *96*, 224502 (1−4).
(32) He, Y.; Gillespie, D.; Boda, D.; Vlassiouk, I.; Eisenberg, R. S.; Siwy, Z. S. Tuning Transport Properties of Nanofluidic Devices with Local Charge Inversion. *J. Am. Chem. Soc.* **2009**, *131*, 5194−5202.
(33) Aguilella-Arzo, M.; Calero, C.; Faraudo, J. Simulation of Electrokinetics at the Nanoscale: Inversion of Selectivity in a Bio-Nanochannel. *Soft Matter* **2010**, *6*, 6079−6082.
(34) García-Giménez, E.; Alcaraz, A.; Aguilella, V. M. Overcharging Below the Nanoscale: Multivalent Cations Reverse the Ion Selectivity of a Biological Channel. *Phys. Rev. E* **2010**, *81*, 021912 (1−7).
(35) García-Giménez, E.; López, M. L.; Aguilella, V. M.; Alcaraz, A. Linearity, Saturation and Blocking in a Large Multiionic Channel: Divalent Cation Modulation of the OmpF Porin Conductance. *Biochem. Biophys. Res. Commun.* **2011**, *404*, 330−334.
(36) Verdiá-Báguena, C.; Queralt-Martín, M.; Aguilella, V. M.; Alcaraz, A. Protein Ion Channels as Molecular Ratchets. Switchable Current Modulation in Outer Membrane Protein F Porin Induced by Millimolar La^{3+} Ions. *J. Phys. Chem. C* **2012**, *116*, 6537−6542.
(37) Besteman, K.; Zevenberger, M. A. G.; Heering, H. A.; Lemay, S. G. Direct Observation of Charge Inversion by Multivalent Ions as as Universal Electrostatic Phenomenon. *Phys. Rev. Lett.* **2004**, *93*, 170802 (1−4).
(38) Besteman, K.; Zevenberger, M. A. G.; Lemay, S. G. Charge Inversion by Multivalent Ions: Dependence on Dielectric Constant and Surface-Charge Density. *Phys. Rev. E* **2005**, *72*, 061501 (1−9).
(39) Valisko, M.; Boda, D.; Gillespie, D. Selectove Adsorption of Ions with Different Diameter and Valence at Highly Charged Surfaces. *J. Phys. Chem. C* **2007**, *111*, 15575−15585.
(40) Bhattacharya, S.; Muzard, J.; Payet, L.; Mathé, J.; Bockelmann, U.; Aksimentiev, A.; Viasnoff, V. Rectification of the Current in α-Hemolysin Pore Depends on the Cation Type: The Alkali Series Probed by Molecular Dynamics Simulations and Experiment. *J. Phys. Chem. C* **2011**, *115*, 4255−4264.
(41) Kowalczyk, S. W.; Wells, D. B.; Aksimentiev, A.; Dekker, C. Slowing Down DNA Translocation through a Nanopore in Lithium Chloride. *Nano Lett.* **2012**, *12*, 1038−1044.
(42) Cervera, J.; Schiedt, B.; Neumann, R.; Mafe, S.; Ramirez, P. Ionic Conduction, Rectification, and Selectivity in Single Conical Nanopores. *J. Chem. Phys.* **2006**, *124*, 104706 (1−9).
(43) White, H. S.; Bund, A. Ion Current Rectification at Nanopores in Glass Membranes. *Langmuir* **2008**, *24*, 2212−2218.
(44) Constantin, D.; Siwy, Z. S. Poisson Nernst-Planck Model of Ion Current Rectification Through a Nanofluidic Diode. *Phys. Rev. E* **2007**, *76*, 041202 (1−10).
(45) Cervera, J.; Alcaraz, A.; Schiedt, B.; Neumann, R.; Ramírez, P. Asymmetric Selectivity of Synthetic Conical Nanopores Probed by Reversal Potential Measurements. *J. Phys. Chem. C* **2007**, *111*, 12265−12273.
(46) Ramírez, P.; Gómez, V.; Cervera, J.; Schiedt, B.; Mafé, S. Ion Transport and Selectivity in Nanopores with Spatially Inhomogeneous Fixed Charge Distributions. *J. Chem. Phys.* **2007**, *126*, 194703 (1−9).
(47) Vlassiouk, I.; Kozel, T.; Siwy, Z. S. Biosensing with Nanofluidic Diodes. *J. Am. Chem. Soc.* **2009**, *131*, 8211−8220.
(48) Cruz-Chu, E. R.; Ritz, T.; Siwy, Z. S.; Schulten, K. Molecular Control of Ionic Conduction in Polymer Nanopores. *Faraday Discuss.* **2009**, *143*, 47−62.
(49) Fleischer, R. L.; Price, P. B.; Walker, R. M. *Nuclear Tracks in Solids: Principles and Applications*; University of California Press: Berkeley, CA, 1975.
(50) Spohr, R. Methods and Device to Generate a Predetermined Number of Ion Tracks. German Patent DE2951376 C2, 15 Sept 1983; US Patent 4369370, 1983.
(51) Phillips, J. C.; et al. Scalable Molecular Dynamics with NAMD. *J. Comput. Chem.* **2005**, *26*, 1781−1802.
(52) Brooks, B. R.; et al. CHARMM: The Biomolecular Simulation Program. *J. Comput. Chem.* **2009**, *30*, 1545−1615.

(53) Yoo, J.; Aksimentiev, A. Improved Parameterization of Li^+, Na^+, K^+, and Mg^+ Ions for All-Atom Molecular Dynamics Simulations of Nucleic Acid Systems. *Phys. Chem. Lett.* **2012**, *3*, 45−50.
(54) Koopman, E. A.; Lowe, C. P. Advantages of a Lowe-Andersen Thermostat in Molecular Dynamics Simulations. *J. Chem. Phys.* **2006**, *123*, 204103 (1−5).
(55) Jorgensen, W. L.; Chandrasekhar, J.; Madura, J. D.; Impey, R. W.; Klein, M. L. Comparison of Simple Potential Functions for Simulating Liquid Water. *J. Chem. Phys.* **1983**, *79*, 926−935.
(56) Martyna, G. J.; Tobias, D. J.; Klein, M. L. Constant Pressure Molecular Dynamics Algorithms. *J. Chem. Phys.* **1994**, *101*, 4177−4189.
(57) Wei, J.; Delgado, R.; Hawley, M. C.; Demeuse, M. T. Dielectric Analysis of Semi-Crystalline Poly(Ethylene Terephthalate). *Mater. Res. Soc. Symp. Proc.* **1994**, *347*, 735−741.
(58) Humphrey, W.; Dalke, A.; Schulten, K. VMD: Visual Molecular Dynamics. *J. Mol. Graphics* **1996**, *14*, 33−38.
(59) Wolf, A.; Reber, N.; Apel, P. Yu.; Fischer, B. E.; Spohr, R. Electrolyte Transport in Charged Single Ion Track Capillaries. *Nucl. Instrum. Methods Phys. Res., Sect. B* **1995**, *105*, 291−293.
(60) Stein, D.; Kruithof, M.; Dekker, C. Surface-Charge-Governed Ion Transport in Nanofluidic Channels. *Phys. Rev. Lett.* **2004**, *93*, 035901−035905.
(61) Wolf-Reber, A. Ph.D. Thesis. Aufbau eines Rasterionenleitwert-mikroskops: Stromfluktuationen von Nanoporen, University of Frankfurt, Frankfurt, Germany, 2002.
(62) Powell, M. R.; Vlassiouk, I.; Martens, C.; Siwy, Z. S. Non-Equilibrium 1/f Noise in Rectifying Nanopores. *Phys. Rev. Lett.* **2009**, *103*, 248104 (1−4).
(63) Liu, J.; et al. Surface Charge Density Determination of Single Conical Nanopores Based on Normalized Ion Current Rectification. *Langmuir* **2012**, *28*, 1588−1595.
(64) Powell, M. R.; Sa, N.; Davenport, M.; Healy, K.; Vlassiouk, I.; Letant, S. E.; Baker, L. A.; Siwy, Z. S. Noise Properties of Rectifying Nanopores. *J. Phys. Chem. C* **2011**, *115*, 8775−8783.
(65) Siwy, Z.; Fulinski, Z. Origin of $1/f^{\alpha}$ Noise in Membrane Channel Currents. *Phys. Rev. Lett.* **2002**, *89*, 158101 (1−4).
(66) Laohakunakorn, N.; Gollnick, B.; Moreno-Herrero, F.; Aarts, D. G. A. L.; Dullens, R. P. A.; Ghosal, S.; Keyser, U. F. A Landau−Squire Nanojet. *Nano Lett.* **2013**, *13*, 5141−5146.
(67) Vlassiouk, I.; Smirnov, S.; Siwy, Z. S. Nanofluidic Ionic Diodes. Comparison of Analytical and Numerical Solutions. *ACS Nano* **2008**, *2*, 1589−1602.
(68) Korchev, Y. E.; Alder, G. M.; Bakhramov, A.; Bashford, C. L.; Joomun, B. S.; Sviderskaya, E. V.; Usherwood, P. N. R.; Pasternak, C. A. Staphylococcus Aureus a-Toxin-Induced Pores: Channel-Like Behavior in Lipid Bilayers and Patch Clamped Cells. *J. Membr. Biol.* **1995**, *143*, 143−151.
(69) Krasilnikov, O. V.; Sabirov, R. Z. Ion Transport through Channels Formed in Lipid Bilayers by Staphylococcus Aureus a-Toxin. *Gen. Physiol. Biophys.* **1989**, *8*, 213−222.
(70) Noskov, S. Yu.; Im, W.; Roux, B. Ion Permeation through the a-Hemolysin Channel: Theoretical Studies Based on Brownian Dynamics and Poisson-Nernst-Plank Electrodiffusion Theory. *Biophys. J.* **2004**, *87*, 2299−2309.
(71) Aksimentiev, A.; Schulten, K. Imaging a-Hemolysin with Molecular Dynamics: Ionic Conductance, Osmotic Permeability, and the Electrostatic Potential Map. *Biophys. J.* **2005**, *88*, 3745−3761.
(72) Lide, D. R., Ed.; *CRC Handbook of Chemistry and Physics*, 94th ed.; CRC Press: Boca Raton, FL, 2013; Section 5.
(73) Squires, T. M.; Bazant, M. Z. Induced-Charge Electro-Osmosis. *J. Fluid Mech.* **2004**, *509*, 217−252.
(74) Rubinstein, I.; Zaltzman, B. Electro-Osmotically Induced Convection at a Permselective Membrane. *Phys. Rev. E* **2000**, *62*, 2238−2251.
(75) Wang, Y.-C.; Stevens, A. L.; Han, J. Million-Fold Preconcentration of Proteins and Peptides by Nanofluidic Filter. *Anal. Chem.* **2005**, *77*, 4293−4299.
(76) Dukhin, S. S. Electrokinetic Phenomena of the Second Kind and Their Applications. *Adv. Colloid Interface Sci.* **1991**, *35*, 173−196.